

Atom scattering as a quantitative surface probe: Noble-gas monolayer and bilayer adsorbed on graphite

H. Jónsson and J. H. Weare

Chemistry Department, University of California at San Diego, La Jolla, California 92093

T. H. Ellis, G. Scoles, and U. Valbusa*

Centre for Molecular Beams and Laser Chemistry, University of Waterloo, Waterloo, Ontario N2L 3G1, Canada

(Received 26 March 1984)

Excellent agreement is found between measured and calculated H-atom scattering by (strongly corrugated) Xe overlayers on graphite. Elastic scattering is calculated exactly using a surface potential generated by summing gas-phase H-Xe potentials. The diffraction peaks are carefully simulated by convolution over the velocity distribution, correcting for inelasticity and geometric effects, and including an inelastic background generated by a new method. Thresholds are found to affect strongly the resonance data, and the behavior of resonances at some crossings is different from that seen in weakly corrugated systems.

Light-atom scattering has been proposed as a very sensitive technique for determining surface structure (see, e.g., Ref. 1). Unlike the probes of other diffraction techniques [e.g., low-energy electron diffraction (LEED)] the atom does not penetrate the outermost layer. This simplifies the interpretation of the data and makes the scattering sensitive to the structure of the surface layer only. Any diffraction technique that is sensitive to the surface can give the size of the surface unit cell from the position of diffraction peaks, as is commonly done with LEED. But the structure within the unit cell can only be determined from the diffraction data by analyzing the heights of the diffraction peaks. Presently this cannot be readily done for any technique, yielding the result that only in a few cases has nontrivial surface structure been solved.

The problem of relating measured diffraction to surface structure is twofold: First, a probe-surface interaction potential must be generated given some configuration of the surface atoms. Second, given this potential, a scattering calculation realistic enough for a meaningful comparison with experimental data needs to be done. In this paper we address the second part. We want to demonstrate that for light-atom scattering this can be done and to illustrate what effects need to be included in the scattering calculation. Previously, good agreement has often been obtained between calculated and measured scattering from weakly corrugated surfaces. But in all cases the atom-surface potential was adjusted to fit the data. Some progress has been made in trying to generate the potential for clean metal surfaces (see, e.g., Ref. 2), but the most important parameter, the surface-corrugation amplitude, cannot be predicted. To minimize the number of unknowns, we study a system that is special in that the surface potential is quite well known, namely the scattering of H atoms from Xe overlayers on graphite. The lattice constant is the only unknown parameter in the scattering calculation and is adjusted to make the position of calculated diffraction peaks agree with the measured ones. (There are, furthermore, two parameters in fitting the background). Peak heights and shapes are found to be sensitive to 1%

changes in lattice constant, illustrating the sensitivity of light-atom scattering to structural features. This system is, furthermore, strongly corrugated and we particularly identify some complications arising because of that. Although many interesting surfaces are strongly corrugated [e.g., Au(110), GaAs(110), Si(110)-(7×7), and Si(111)], good agreement between calculation and data for such systems has not been obtained previously. There are basically two different kinds of data: resonance data and diffraction data. We show that both are accurately predicted from our assumed potential.

Resonance data for weakly corrugated surfaces have previously provided valuable information about the atom-surface interaction potential. The bound states of the laterally averaged potential can be inferred from the position of isolated resonance features and the corrugation (and therefore structural information) from the splitting of resonances at crossings. In analyzing such data it is necessary to identify and assign the observed resonance features. In strongly corrugated systems these features are broad and usually not isolated, making the assignment difficult. An understanding of the resonance behavior is therefore valuable. We identify some new effects that are not seen in data for weakly corrugated surfaces.

The characteristics of the apparatus³ and the layer-growing procedures^{4,5} have been given elsewhere. The Xe layers are not in thermodynamic equilibrium and therefore cannot easily be compared to those studied previously using other techniques.⁶

The theoretical calculation was carried out as follows. Assuming that the surface is perfectly periodic and rigid, the scattering probability for an incident plane wave can be calculated exactly using close-coupling methods.⁷ 130 Fourier components (channels) were included in the periodic part of the wave function to obtain convergence. Typically half of these are open channels (diffracted outgoing beams), but the remaining half are closed channels (evanescent waves). The computer time was significantly reduced by taking account of symmetry and special properties of the surface potential. Only 61 Fourier com-

ponents of the potential need to be included, some of which extend only a short distance out from the surface.

The two-body Xe-H potential has previously been determined by gas-phase scattering experiments.⁸ Since the interaction of the Xe atoms with the underlying substrate (graphite) is weak, the H-adlayer potential is calculated by summing two-body potentials. The zero Fourier component (lateral average) of the true surface potential also contains the long-range hydrogen graphite attraction and long-range three-body interactions. The former is included as $-C_3/(z-z_0)^3$ using literature values for clean graphite.⁴ The uncertainty in this could cause an error in the well depth on the order of 1 meV (5%). This will affect the position of resonance features. But, because the diffraction probability is convoluted over the rather wide energy distribution in the incident beam, the diffraction peaks are not very sensitive to this uncertainty. The bound states of this potential agree to within 5% with those determined from resonance data. This places a constraint on the magnitude of three-body contributions, which are not included. We note, however, that small changes in the well depth of the two-body H-Xe potential lead to large changes in the well depth of the surface potential.

As of yet there is no proven way of correcting calculated elastic intensities for inelastic effects. Because of multiple scattering a Debye-Waller approach does not have as sound theoretical justification as in x-ray or neutron scattering. On the other hand, theoretical results suggest that this approach works best for light projectile atoms and low energy.⁹ Here we use Debye-Waller (DW) corrections determined by independent measurements of the temperature dependence of the specular intensity.⁵ The validity of this approach is supported by good agreement between the mean displacement of Xe atoms found by hydrogen scattering and results of LEED measurements.⁵

Finally, in order to compare the calculation with the data, a convolution of the scattering probabilities over the velocity distribution in the incident beam is carried out. Commonly the reverse procedure is followed, i.e., deconvoluted data are reported. In the present case this is not possible. Because of the large surface corrugation, many closed channels are strongly coupled to the incident beam and the effects of resonances and thresholds cause the diffraction probabilities to vary strongly with energy. Even at normal incidence the diffraction probabilities oscillate rapidly with energy, often changing by a factor of 2 over 1 meV. This can affect the position of the peak maximum so that the lattice constant cannot be reliably determined from the experimental peak positions alone. Therefore, the scattering experiment has to be simulated and the result compared to the data. The calculated detector signal is

$$S(\theta) = p \sum_n \int dk D_n(k) P_n(k) f(k) A_n(k, \theta) + b(\theta),$$

where D_n is the Debye-Waller factor and P_n is the elastic transition probability for diffraction peak n . f is the wave-vector probability distribution [here $\Delta k/k = 14\%$ full width at half maximum (FWHM)] and A is the frac-

tion of outgoing beam n that overlaps with the detector. It is important to recognize that the different outgoing beams have different cross-sectional area. This leads to a geometric correction, even for a perfectly monochromatic beam. The background is represented by a smooth function $b(\theta)$ which is constructed by assuming, in accordance with approximate theoretical results,⁹ that the inelastic scattering removed from each peak by the DW correction is distributed in a broad peak under it. We choose a Gaussian distribution with decay length d_n and height $\alpha d_n^{-1}(1-D_n)P_n$. The decay length, d_n , is the sum of the half-width of elastic peak n due to the spread in velocity (0° – 10°) and an inelastic term. The inelastic term (19°) and α are the same for all peaks and are fitted to the experimental background. This two-parameter fit to the background works well for different incoming angles. In order to ascertain the validity of this approach we have applied it to the energy-selected data for Ne scattering from LiF.¹⁰ The inelastic scattering deduced from the elastic scattering as described above is in good agreement with the measured inelastic scattering, except for very large outgoing angles ($\theta > 70^\circ$). Since the inelastic background is a common problem in analyzing atom-surface scattering data, this is an encouraging result.

In Figs. 1(a)–(c) calculated results are compared to experimental data for a Xe monolayer. Initially we assumed that the Xe layer formed a $\sqrt{3} \times \sqrt{3}$ lattice in registry with the graphite substrate (lattice constant $a = 4.26$ Å). As can be seen in Fig. 1(a) this makes the higher-order diffraction peaks too small and their position is too far from the specular peak. It was clear from these as well as data taken at normal incidence that the lattice constant of the Xe layer is larger. Excellent agreement was obtained by increasing it to $a = 4.34$ Å as is shown in Fig. 1(b). The shape of the diffraction peaks as well as their position and size are all well reproduced by the simulation. The large shoulder on the (1,0) peak is due to larger elastic diffraction probability at lower energy. This illustrates well the need to simulate the data. Similar behavior has been observed when He is scattered from Xe on graphite.¹¹ In this diffraction scan the convolution effects and the inelastic correction change the relative peak heights by as much as a factor of 4 and 2, respectively.

Figure 1(c) shows the effect of changing the two-body H-Xe potential in an effort to fit the diffraction peaks, keeping the lattice constant at $a = 4.26$ Å. We found the distance, σ , to the zero of the two-body potential to be the important parameter. By decreasing σ by 2% the peak heights were made to agree with the data but the peak positions are consistently too far from the specular peak, showing that the lattice constant is too small.

Figure 2 shows measured and calculated diffraction when two layers (a bilayer) of Xe are adsorbed on the graphite. Since the Xe-H two-body and three-body forces are the same as for the monolayer, the measured difference in diffraction peak heights can only be due to a difference in the inelastic scattering and a different lattice constant. The best agreement, shown in Fig. 2, was obtained with a larger lattice constant, $a = 4.40$ Å. The background is different from the monolayer background because of changes in DW factor and elastic intensity. It

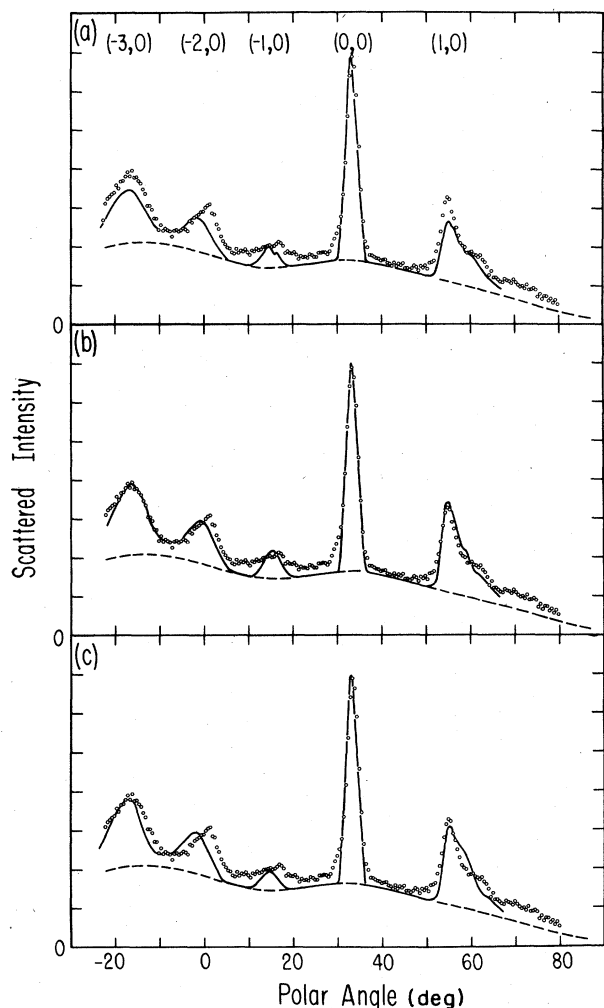


FIG. 1. Measured and calculated scattering from a monolayer of Xe. $k = 6.15 \text{ \AA}^{-1}$, $T = 13 \text{ K}$, $\theta_i = 33.2^\circ$. (a) Pair potential from gas-phase measurements, $a = 4.26 \text{ \AA}$. (b) Same pair potential, $a = 4.34 \text{ \AA}$. (c) Adjusted pair potential, $a = 4.26 \text{ \AA}$. All calculations use the same background which was deduced from calculation (b).

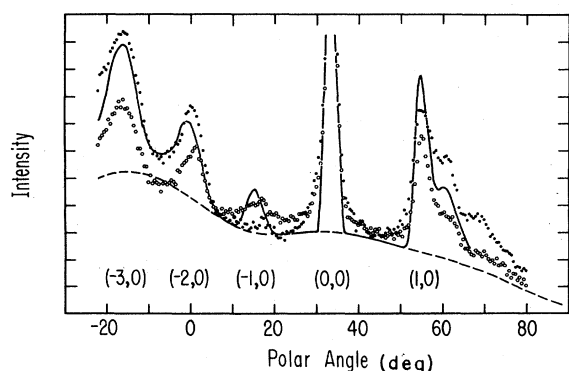


FIG. 2. Measured scattering from a bilayer of Xe (filled circles) and the monolayer data from Fig. 1 (open circles). The experimental conditions are the same in both cases. Solid line shows calculated results using $a = 4.40 \text{ \AA}$. The (0,0) peak has the same height in all cases.

is constructed in the same way as for the monolayer, adjusting only α . The increased height of the $(-3,0)$ peak over the overlap region (at $\theta = -10^\circ$) is well reproduced by the calculation as well as the appearance of a second maximum in the $(1,0)$ beam.

Calculated and measured resonance structure in the specular scattering from a Xe monolayer is compared in Fig. 3. By gradually reducing the corrugation in our calculation we have determined that the resonance features in Fig. 3 satisfy the rules originally derived by Wolfe and Weare¹² for weakly corrugated surfaces. At the threshold of the $(-1,0)$ channel there is an abrupt change in the direct scattering (nonresonant) contribution to the specular intensity (at $\phi = 85.6^\circ$) and the $(1,0)$ and $(-1,0)$ resonances are minima coming down from the higher baseline. Because of this prior assignment of resonance features in the data were incorrect.¹³ An approximate averaging over the energy distribution was carried out by assuming that each resonance feature has the same shape at a different energy but is found at a different angle. The displacement was taken to be proportional to the difference in wave vector. The proportionality constant was determined from calculated resonance positions distributed around the mean energy. As can be seen from Fig. 3, the narrow feature at the threshold, which moves rapidly with energy, is averaged out.

The resonance data also provide information about the corrugation of the surface. The $(-1,0)$ and the $(1,0)$ resonances are split about the symmetry direction, $\phi = 90^\circ$. Figure 3 shows the closest approach of the two minima where their positions change only slowly with energy. The calculation shown assumes that the monolayer is in registry ($a = 4.27 \text{ \AA}$) and predicts too small a splitting because the corrugation is too small. When the lattice constant is increased to get agreement with diffraction data, the position of this minimum moves to the experimental position.

The behavior of this splitting is qualitatively different from that expected from band-structure calculations as used previously in analyzing data for weakly corrugated surfaces.¹⁴ These predict the trajectories of the minima to

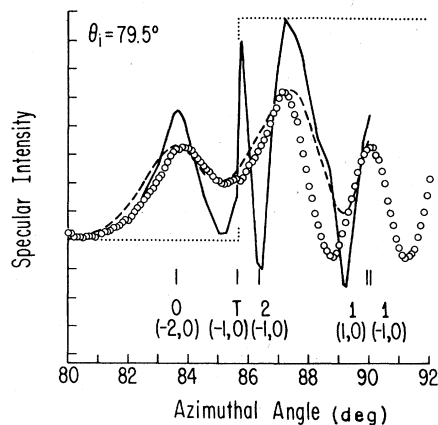


FIG. 3. Measured resonance structure in the $(0,0)$ beam (open circles). Solid line: calculated intensity for $k = 6.25 \text{ \AA}^{-1}$. Dashed line: energy averaged intensity. Dotted line indicates the direct scattering baseline. $\phi = 90^\circ$ is a symmetry direction.

cross the symmetry line. At this crossing direct coupling between the two resonances (through the V_{02} Fourier component) is weak compared to second-order coupling through continuum states. In weakly corrugated systems this splitting is too small to be seen. A second-order perturbation¹² calculation including the continuum states in the pole approximation gives the right behavior and a closest approach at $\phi=89.0^\circ$, in reasonable agreement with the exact calculation.

To summarize, the good agreement obtained here between experimental data and a calculation based on a known surface potential demonstrates that even for strongly corrugated surfaces the scattering of light atoms can be calculated accurately enough for this technique to

give detailed structural information. It can be important to convolute the calculation instead of deconvoluting data, especially for strongly corrugated surfaces. Geometric effects as well as inelastic corrections must be included and a simple rule for generating the inelastic background can be used. A different kind of splitting of resonances can be expected and thresholds are an important consideration when data for strongly corrugated surfaces are analyzed.

This work was supported in part by the National Science Foundation under Grant No. INT80-19908 and Consiglio Nazionale delle Ricerche CNRn 22.CT/81.00522.02/115.1827.

*Permanent address: Physics Department, University of Genova, 16133 Genova, Italy.

¹K. H. Rieder and T. Engel, *Phys. Rev. Lett.* **45**, 824 (1980).

²J. Harris and A. Liebsch, *Phys. Rev. Lett.* **49**, 341 (1982).

³G. Caracciolo, S. Iannotta, G. Scoles, and U. Valbusa, *J. Chem. Phys.* **72**, 4491 (1980).

⁴T. H. Ellis, S. Iannotta, G. Scoles, and U. Valbusa, *Phys. Rev. B* **24**, 2304 (1981).

⁵T. H. Ellis, G. Scoles, and U. Valbusa, *Chem. Phys. Lett.* **94**, 247 (1983).

⁶P. S. Schabes-Retchkiman and J. A. Venables, *Surf. Sci.* **105**, 536 (1981).

⁷W. N. Sams and D. J. Kouri, *J. Chem. Phys.* **51**, 4809 (1969); **52**, 4144 (1970).

⁸J. P. Toennies, W. Welz, and G. Wolf, *J. Chem. Phys.* **71**, 614 (1979).

⁹A. C. Levi and H. Suhl, *Surf. Sci.* **88**, 221 (1979); A. C. Levi, *Nuovo Cimento* **54**, 357 (1979).

¹⁰L. Mattera, C. Salvo, S. Terreni, F. Tommasini, and U. Valbusa, *Surf. Sci.* **124**, 571 (1983).

¹¹P. Cantini (private communication).

¹²K. L. Wolfe and J. H. Weare, *Phys. Rev. Lett.* **41**, 1663 (1978).

¹³T. H. Ellis, G. Scoles, and U. Valbusa, *Surf. Sci.* **118**, L251 (1982).

¹⁴G. P. Boato, P. Cantini, C. Guidi, R. Tatarek, and G. P. Felcher, *Phys. Rev. B* **20**, 3957 (1979); H. Chow and E. D. Thompson, *Surf. Sci.* **59**, 225 (1976).